Parameter Estimation and Beam Tracking in Integrated Sensing and Communication System

Ruotong Xu, Chenhao Qi and Kangjian Chen
National Mobile Communications Research Laboratory
School of Information Science and Engineering, Southeast University, Nanjing, China
Email: {213180979, qch, kjchen}@seu.edu.cn

2022 IEEE 96th Vehicular Technology Conference (VTC2022-Fall) | 978-1-6654-5468-1/22/$31.00 ©2022 IEEE | DOI: 10.1109/VTC2022-Fall57202.2022.10012934

***Abstract*—In this paper we investigate the uplink collaborative sensing in the mmWave MIMO integrated sensing and communication system. Since the vehicles periodically transmit pilot sequences to the road side unit (RSU) and the pilot sequences are *a priori* knowledge of the RSU, the RSU can perform collaborative sensing and parameter estimation for the vehicles. A two-dimensional fast Fourier transform (FFT) and estimating-signal-parameter-via-rotational-invariance-techniques (ESPRIT)-based scheme is proposed for parameter estimation in the RSU, where the FFT is used to estimate the distance and relative radial velocity, and the ESPRIT is used to estimate the angle-of-arrival and angle-of-departure of the channel line-of-sight path. Then these estimated parameters are exploited by an extended Kalman filtering model to achieve the efficient beam tracking. Simulation results verify the effectiveness of the proposed scheme and show that it can save the estimation resources while ensuring the estimation accuracy.**

***Index Terms*—Beam tracking, collaborative sensing, integrated sensing and communication (ISAC), parameter estimation.**

I. Introduction

Wireless communication and radar sensing have been evolved independently in different frequency spectrums and systems all the time. But recently, the spectrum scarcity and the environmental complexity have raised the rethink of efficient utilization of the spectral and hardware resources, and have promoted extensive research on integrated sensing and communication (ISAC) [1].

In the ISAC system, wireless communication and radar sensing can share the same signal processing modules and frequency spectrum, and therefore greatly improve the spectrum and hardware utilization. In [2], radar-communication coexistence is achieved through orthogonal frequency division multiplexing (OFDM), where the radar signal is modulated on idle OFDM subcarriers. Aiming at approaching the desired radar beam pattern, MIMO beamforming is designed for a base station with dual functions of radar sensing and communication, subject to the power constraints and signal-to-interference-plus-noise ratio for communication users [3]. Different from the ISAC system supported by a single beam, a multibeam design scheme using analog antenna arrays to simultaneously generate a communication subbeam and a sensing subbeam is proposed, where the communication subbeam is fixed to achieve stable wireless communications and the sensing subbeam is time-varying to scan the environment [4].

Since the ISAC system can benefit from the collaboration between radar sensing and wireless communications, it provides a promising platform for the vehicle to everything (V2X) network [5]. In the V2X network, low-latency wireless communications and high-resolution sensing are required to ensure the quality of service for the vehicles with high mobility. To satisfy the above requirement, a radar-assisted predictive beamforming scheme is proposed, where the road side unit (RSU) first sends ISAC signal to vehicles for simultaneously communication and sensing, and then estimates the wireless channels based on ISAC echoes and designs the beamforming based on predicted angles [6]. Nonetheless, the existing works mainly focus on the sensing and estimation using ISAC echoes, which cannot efficiently highlight the targets from the environment or distinguish different targets.

In this paper, we investigate the uplink collaborative sensing in the mmWave MIMO ISAC system. Since the vehicles periodically transmit pilot sequences to the RSU and the pilot sequences are *a priori* knowledge of the RSU, the RSU can perform collaborative sensing and parameter estimation for the vehicles. A two-dimensional fast Fourier transform (FFT) and estimating-signal-parameter-via-rotational-invariance-techniques (ESPRIT)-based scheme is proposed for parameter estimation in the RSU, where the FFT is used to estimate the distance and relative radial velocity, and the ESPRIT is used to estimate the angle-of-arrival (AoA) and angle-of-departure (AoD) of the channel line-of-sight (LoS) path. Then these estimated parameters are exploited by an extended Kalman filtering (EKF) model to achieve the efficient beam tracking.

The rest of the paper is arranged as follows. Section II introduces the system model for uplink collaborative sensing. Section III proposes a two-dimensional FFT and ESPRIT-based parameter estimation scheme, and then applies it to EKF beam tracking. The simulation results are provided in Section IV. Finally, Section V concludes the paper.

Notations: For a vector $\boldsymbol{a}$, $(\boldsymbol{a})_m$ and $\mathrm{diag}\{\boldsymbol{a}\}$ denote the mth entry of $\boldsymbol{a}$ and a diagonal matrix with the entries of $\boldsymbol{a}$ on the main diagonal, respectively. For a matrix $\boldsymbol{A}$, $(\boldsymbol{A})_{m,n}$, $\|\boldsymbol{A}\|_F$, $\boldsymbol{A}^T$ and $\boldsymbol{A}^H$ denote the entry on the mth row and nth column, Frobenius norm, transpose and Hermitian of $\boldsymbol{A}$, respectively. The symbols $\boldsymbol{I}_L$, $\mathbb{R}^{M\times N}$ and $\mathbb{C}^{M\times N}$ denote an $L\times L$ identity matrix, the set of $M\times N$ real-valued matrices and the set of $M\times N$ complex-valued matrices, respectively.

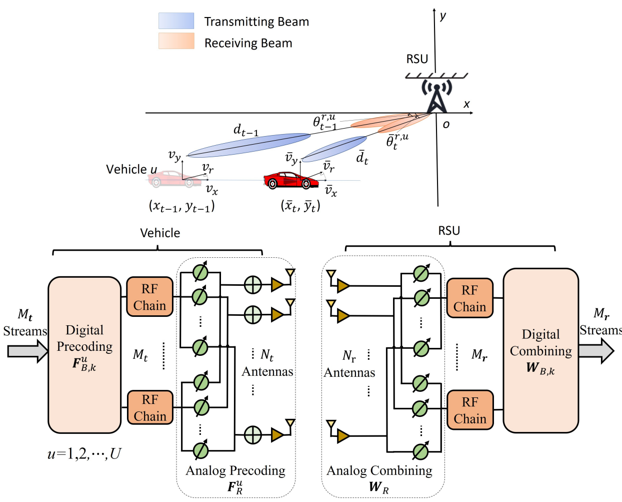

Fig. 1. Block diagram of an mmWave MIMO ISAC system.

The function $\mathbb{E}\{\cdot\}$ denotes the expectation.

II. System Model

As shown in Fig. 1, we consider an mmWave MIMO ISAC system, including a RSU and U vehicles. OFDM modulation is employed to deal with the frequency-selective fading. Let N_r, N_t, M_r and M_t denote the numbers of antennas at the RSU and at each vehicle and the numbers of radio frequency (RF) chains at the RSU and at each vehicle, respectively. The antennas at both sides are placed in uniform linear arrays with half wavelength intervals. The hybrid precoding and hybrid combining are employed in the system [7], where the number of RF chains is much smaller than that of antennas, i.e., $M_r \ll N_r$, $M_t \ll N_t$. During the uplink transmission from vehicles to the RSU, the received signal at the kth subcarrier of the bth block can be represented as

$$\boldsymbol{y}_{k,b} = \boldsymbol{W}_{B,k}\boldsymbol{W}_R \sum_{u=1}^{U} \boldsymbol{H}_{k,b}^u \boldsymbol{F}_R^u \boldsymbol{F}_{B,k}^u \boldsymbol{s}_{k,b}^u + \boldsymbol{W}_{B,k}\boldsymbol{W}_R \boldsymbol{n}, \quad (1)$$

where $\boldsymbol{F}_{B,k}^u \in \mathbb{C}^{M_t \times M_t}$, $\boldsymbol{F}_R^u \in \mathbb{C}^{N_t \times M_t}$, $\boldsymbol{W}_{B,k} \in \mathbb{C}^{M_r \times M_r}$ and $\boldsymbol{W}_R \in \mathbb{C}^{M_r \times N_r}$ denote the digital precoding matrix, analog precoding matrix, digital combining matrix and analog combining matrix for the uth vehicle, respectively. We set $||\boldsymbol{W}_{B,k}\boldsymbol{W}_R||_F^2 = 1$ and $||\boldsymbol{F}_R^u \boldsymbol{F}_{B,k}^u||_F^2 = 1$ to make sure that the powers of hybrid precoder and combiner are normalized. Let $\boldsymbol{H}_{k,b}^u \in \mathbb{C}^{N_r \times N_t}$, $\boldsymbol{s}_{k,b}^u \in \mathbb{C}^{M_t \times N_s}$ and $\boldsymbol{n} \in \mathbb{C}^{N_r \times N_s}$ denote the uplink sensing channel matrix at the kth subcarrier of the bth block between the RSU and the uth vehicle, the signal matrix and the additive white Gaussian noise (AWGN) matrix with each column satisfying independent complex Gaussian distribution with zero mean and variance σ^2, respectively, where N_s denotes the number of OFDM symbols in a block.

According to [1], the frequency domain time-varying uplink sensing channel matrix in (1) can be expressed as

$$\boldsymbol{H}_{k,b}^u = \sqrt{N_t N_r / L} \sum_{l=1}^{L} b_l e^{-j2\pi k \Delta f \tau_l^u} e^{j2\pi f_{D,l}^u b T_b} \cdot \boldsymbol{\alpha}\left(N_r, \theta_l^{r,u}\right) \boldsymbol{\alpha}^H \left(N_t, \theta_l^{t,u}\right), \quad (2)$$

where L, Δf and T_b denote the number of the resolvable paths, the subcarrier interval and the time duration of a block, respectively. Let b_l, τ_l^u and $f_{D,l}^u$ denote the complex gain, propagation delay and Doppler frequency offset of the lth path, respectively. For the uplink sensing, $\tau_l^u = d_l^u / c$ and $f_{D,l}^u = v_l^u f_c / c$, where d_l^u, v_l^u, f_c and c denote the propogation distance, the relative radial velocity of the uth vehicle, the central subcarrier frequency of OFDM and the speed of light, respectively. The steering vector is denoted as

$$\boldsymbol{\alpha}(N, \theta) = 1/\sqrt{N}[1, e^{j\pi\theta}, e^{j\pi d 2\theta}, \cdots, e^{j\pi d (N-1)\theta}]^T. \quad (3)$$

The angle-of-arrival (AoA) and angle-of-departure (AoD) of the lth path are denoted as $\vartheta_l^{u,r}$ and $\vartheta_l^{u,t}$, respectively, and then in (2), $\theta_l^{r,u} \triangleq \sin(\vartheta_l^{r,u})$ and $\theta_l^{t,u} \triangleq \sin(\vartheta_l^{t,u})$. Thus we can rewrite (2) in a more compact form as

$$\boldsymbol{H}_{k,b}^u = \gamma \boldsymbol{A}_R^u \Delta_{k,b}^u (\boldsymbol{A}_T^u)^H, \quad (4)$$

where $\gamma \in \mathbb{R}^{1\times 1}$, $\boldsymbol{A}_R^u \in \mathbb{C}^{N_r \times L}$, $\boldsymbol{A}_T^u \in \mathbb{C}^{N_t \times L}$ and $\Delta_{k,b}^u \in \mathbb{C}^{L \times L}$ are denoted as

$$\begin{aligned} \gamma &\triangleq \sqrt{N_t N_r / L}, \\ \boldsymbol{A}_R^u &\triangleq [\boldsymbol{\alpha}(N_r, \theta_1^{r,u}), \boldsymbol{\alpha}(N_r, \theta_2^{r,u}), \cdots, \boldsymbol{\alpha}(N_r, \theta_L^{r,u})], \\ \boldsymbol{A}_T^u &\triangleq [\boldsymbol{\alpha}(N_t, \theta_1^{t,u}), \boldsymbol{\alpha}(N_t, \theta_2^{t,u}), \cdots, \boldsymbol{\alpha}(N_t, \theta_L^{t,u})], \\ \Delta_{k,b}^u &\triangleq \mathrm{diag}\{[b_1 e^{-j2\pi k \Delta f \tau_1^u} e^{j2\pi f_{D,1}^u b T_b}, \cdots, \\ &\qquad b_L e^{-j2\pi k \Delta f \tau_L^u} e^{j2\pi f_{D,L}^u b T_b}]\}. \end{aligned} \quad (5)$$

III. Parameter Estimation and Beam Tracking

In this section, we propose a two-dimensional FFT and ESPRIT-based scheme for collaborative sensing and parameter estimation, where the distance and radial velocity are estimated using FFT, and then AoA and AoD of the LoS path are estimated using ESPRIT. The estimated parameters are exploited by EKF to achieve the efficient beam tracking.

A. Parameter Estimation

At the tth epoch of the beam tracking for the uth vehicle, the vehicle and the RSU should choose suitable codewords to transmit and receive signals such that the beamforming gain is maximized. We predefine the codebooks at the vehicles and the RSU as $\boldsymbol{\mathcal{F}}_c \triangleq \{\boldsymbol{f}_c(1), \boldsymbol{f}_c(2), \ldots, \boldsymbol{f}_c(\mathrm{N_t})\}$ and $\boldsymbol{\mathcal{W}}_c \triangleq \{\boldsymbol{w}_c(1), \boldsymbol{w}_c(2), \ldots, \boldsymbol{w}_c(\mathrm{N_r})\}$, respectively, where $\boldsymbol{f}_c(n) \triangleq \boldsymbol{\alpha}\left(\mathrm{N_t}, -1 + (2n-1)/\mathrm{N_t}\right)$, and $\boldsymbol{w}_c(n) \triangleq \boldsymbol{\alpha}\left(\mathrm{N_r}, -1 + (2n-1)/\mathrm{N_r}\right)^H$ denote the nth precoding codeword with beam coverage of $[-1+2(n-1)/\mathrm{N_t}, -1+2n/\mathrm{N_t}]$ and the nth combining codeword with beam coverage of $[-1+2(n-1)/\mathrm{N_r}, -1+2n/\mathrm{N_r}]$, respectively.

We denote the chosen precoding codeword and the combining codeword as $\boldsymbol{f}_c(\tilde{n})$ and $\boldsymbol{w}_c(\tilde{n})$, respectively, which cover the predicted AoA and AoD obtained at the $(t-1)$th epoch. The prediction model will be given in Section III.B.

We define the observation vector for the uth vehicle in the RSU at the tth epoch as

$$\boldsymbol{Z}[t] = [\hat{d}^u_{los}, \hat{\theta}^{r,u}_{los}, \hat{v}^u_{los}]^T, \tag{6}$$

where $\hat{d}^u_{los}$, $\hat{\theta}^{r,u}_{los}$ and $\hat{v}^u_{los}$ denote the estimated distance, AoA and relative radial velocity of the LoS path, respectively.

To get $\boldsymbol{Z}[t]$ in the RSU, vehicles transmit B OFDM blocks periodically to the RSU. Specifically, in each block, each vehicle uses K subcarriers to transmit the pilot sequence through an RF chain for three times. The pilot sequence of the uth vehicle is denoted as $\boldsymbol{p}^u_k \in \mathbb{C}^U$ and satisfies $(\boldsymbol{p}^u_k)^H \boldsymbol{p}^u_k = 1$ and $(\boldsymbol{p}^u_k)^H \boldsymbol{p}^i_k = 0$, $\forall u, i \in \{1, 2, \cdots, U\}$, $u \neq i$. Then the time duration of a block can be computed as $T_b = 3UT_o$, where T_o denotes the time duration of one OFDM symbol.

We divide a block into three stages, each of which contains a pilot sequence. The received pilot sequences at the kth subcarrier of the bth block can be denoted as

$$\boldsymbol{y}^{(i)}_{k,b} = \boldsymbol{w}_c(\tilde{n}) \sum_{u=1}^{U} \boldsymbol{H}^u_{k,b} \boldsymbol{f}_c(\tilde{n}) (\boldsymbol{p}^u_k)^H + \boldsymbol{w}_c(\tilde{n}) \boldsymbol{n}^{(i)}_{k,b}, \tag{7}$$

where $i \in \{1, 2, 3\}$ denotes the index of stage. Let $\boldsymbol{H}^u_{k,b} \in \mathbb{C}^{N_r \times N_t}$ and $\boldsymbol{n}^{(i)}_{k,b} \in \mathbb{C}^{N_r \times U}$ denote the channel matrix and the AWGN matrix at the ith stage of the bth block between the RSU and the uth vehicle, respectively. By multiplying $\boldsymbol{y}^{(i)}_{k,b}$ with $\boldsymbol{p}^u_k$, we have

$$r^{u,(i)}_{k,b} = \boldsymbol{y}^{(i)}_{k,b} \boldsymbol{p}^u_k = \boldsymbol{w}_c(\tilde{n}) \boldsymbol{H}^u_{k,b} \boldsymbol{f}_c(\tilde{n}) + \tilde{n}^{(i)}_{k,b}, \tag{8}$$

where $\tilde{n}^{(i)}_{k,b} \triangleq \boldsymbol{w}_c(\tilde{n}) \boldsymbol{n}^{(i)}_{k,b} \boldsymbol{p}^u_k$. Inspired by [8], to make use of the rotation invariance property of the steering matrix to perform the parameter estimation, we arrange the antenna arrays in different ways at different stages of each block.

At the first stage, the RSU powers off the N_rth antenna and each vehicle powers off the N_tth antenna. Then $\boldsymbol{w}_c(\tilde{n})$ and $\boldsymbol{f}_c(\tilde{n})$ at the first stage can be expressed as

$$\widetilde{\boldsymbol{w}}^{(1)} = [\widetilde{\boldsymbol{w}}_c, 0], \quad \widetilde{\boldsymbol{f}}^{(1)} = [(\widetilde{\boldsymbol{f}}_c)^T, 0]^T, \tag{9}$$

where $\widetilde{\boldsymbol{w}}_c \in \mathbb{C}^{1 \times (N_r - 1)}$ and $\widetilde{\boldsymbol{f}}_c \in \mathbb{C}^{(N_t - 1) \times 1}$ denote $\boldsymbol{w}_c(\tilde{n})$ and $\boldsymbol{f}_c(\tilde{n})$ with $N_r - 1$ and $N_t - 1$ antennas powered on, respectively. Substituting (4) and (9) into (8), we have

$$r^{u,(1)}_{k,b} = \gamma \widetilde{\boldsymbol{w}}_c \boldsymbol{A}^{u,(1)}_R \Delta^u_{k,b} (\boldsymbol{A}^{u,(1)}_T)^H \widetilde{\boldsymbol{f}}_c + \tilde{n}^{(1)}_{k,b}, \tag{10}$$

where $\boldsymbol{A}^{u,(1)}_T \in \mathbb{C}^{(N_t - 1) \times L}$ and $\boldsymbol{A}^{u,(1)}_R \in \mathbb{C}^{(N_r - 1) \times L}$ consist of the first $N_t - 1$ rows and the first $N_r - 1$ rows of $\boldsymbol{A}^u_T$ and $\boldsymbol{A}^u_R$, respectively.

At the second stage, the RSU powers off the first antenna and each vehicle powers off the N_tth antenna. Then $\boldsymbol{w}_c(\tilde{n})$ and $\boldsymbol{f}_c(\tilde{n})$ at the second stage can be expressed as

$$\widetilde{\boldsymbol{w}}^{(2)} = [0, \widetilde{\boldsymbol{w}}_c], \quad \widetilde{\boldsymbol{f}}^{(2)} = [(\widetilde{\boldsymbol{f}}_c)^T, 0]^T, \tag{11}$$

where $\widetilde{\boldsymbol{w}}_c$ and $\widetilde{\boldsymbol{f}}_c$ are the same with that of the first stage. Substituting (4) and (11) into (8), we have

$$r^{u,(2)}_{k,b} = \gamma \widetilde{\boldsymbol{w}}_c \boldsymbol{A}^{u,(2)}_R \Delta^u_{k,b} (\boldsymbol{A}^{u,(2)}_T)^H \widetilde{\boldsymbol{f}}_c + \tilde{n}^{(2)}_{k,b}, \tag{12}$$

Algorithm 1 Two-Dimensional FFT and ESPRIT-based algorithm for Collaborative Sensing and Parameter Estimation

1: **Input:** $\boldsymbol{r}^{u,(1)}_{k,b}$, $\boldsymbol{r}^{u,(2)}_{k,b}$, $\boldsymbol{r}^{u,(3)}_{k,b}$,
$k \in \{1, 2, \cdots, K\}$, $b \in \{1, 2, \cdots, B\}$.
2: Compute $\boldsymbol{P}^{u,(1)}$ via (17).
3: Obtain Ω_d and Ω_v via the search of $\boldsymbol{P}^{u,(1)}$.
4: Compute $\hat{d}^u_{los}$ and $\hat{v}^u_{los}$ via (18).
5: Compute $\boldsymbol{P}^{u,(2)}$ and $\boldsymbol{P}^{u,(3)}$ via two-dimensional FFT.
6: Obtain $\boldsymbol{P}^u$ via (20).
7: Compute $\boldsymbol{B}^u$ via (22).
8: Compute $\boldsymbol{U}$ via (23).
9: Obtain $U_{s,1}$ and $U_{s,2}$ via (24).
10: Compute $\hat{\theta}^{r,u}_{los}$ via (25).
11: Repeat step 6-10 by replacing (27) with (28).
12: **Output:** $\hat{d}^u_{los}$, $\hat{v}^u_{los}$, $\hat{\theta}^{r,u}_{los}$, $\hat{\theta}^{t,u}_{los}$.

where $\boldsymbol{A}^{u,(2)}_T$ is the same with $\boldsymbol{A}^{u,(1)}_T$, and $\boldsymbol{A}^{u,(2)}_R \in \mathbb{C}^{(N_r - 1) \times L}$ consists of the last $N_r - 1$ rows of $\boldsymbol{A}^u_R$.

At the third stage, the RSU powers off the N_rth antenna and each vehicle powers off the first antenna. Then $\boldsymbol{w}_c(\tilde{n})$ and $\boldsymbol{f}_c(\tilde{n})$ at the third stage can be expressed as

$$\widetilde{\boldsymbol{w}}^{(3)} = [\widetilde{\boldsymbol{w}}_c, 0], \quad \widetilde{\boldsymbol{f}}^{(3)} = [0, (\widetilde{\boldsymbol{f}}_c)^T]^T, \tag{13}$$

where $\widetilde{\boldsymbol{w}}_c$ and $\widetilde{\boldsymbol{f}}_c$ are the same with that of the first stage. We substitute (4) and (13) into (8) and have

$$r^{u,(3)}_{k,b} = \gamma \widetilde{\boldsymbol{w}}_c \boldsymbol{A}^{u,(3)}_R \Delta^u_{k,b} (\boldsymbol{A}^{u,(3)}_T)^H \widetilde{\boldsymbol{f}}_c + \tilde{n}^{(3)}_{k,b}, \tag{14}$$

where $\boldsymbol{A}^{u,(3)}_T \in \mathbb{C}^{(N_t - 1) \times L}$ consisits of the last $N_t - 1$ rows of $\boldsymbol{A}^u_T$, and $\boldsymbol{A}^{u,(3)}_R$ is the same with $\boldsymbol{A}^{u,(1)}_R$.

To estimate distance, relative radial velocity, AoA and AoD of the LoS path using $r^{u,(i)}_{k,b}$, we propose a two-dimensional FFT and ESPRIT-based algorithm for collaborative sensing and parameter estimation in the RSU as shown in Algorithm 1. We stack all $r^{u,(1)}_{k,b}$ together and have

$$\boldsymbol{r}^{u,(1)} = \begin{bmatrix} r^{u,(1)}_{1,1} & r^{u,(1)}_{1,2} & \cdots & r^{u,(1)}_{1,B} \\ r^{u,(1)}_{2,1} & r^{u,(1)}_{2,2} & \cdots & r^{u,(1)}_{2,B} \\ \vdots & \vdots & \ddots & \vdots \\ r^{u,(1)}_{K,1} & r^{u,(1)}_{K,2} & \cdots & r^{u,(1)}_{K,B} \end{bmatrix}. \tag{15}$$

Similarly, we can get $\boldsymbol{r}^{u,(2)}$ and $\boldsymbol{r}^{u,(3)}$ by stacking all $\boldsymbol{r}^{u,(2)}_{k,b}$ and $\boldsymbol{r}^{u,(3)}_{k,b}$ together, respectively.

To analyze the property of $\boldsymbol{r}^{u,(1)}$, we rewrite $\boldsymbol{r}^{u,(1)}$ as

$$(\boldsymbol{r}^{u,(1)})_{k,b} = \kappa \sum_{l=1}^{L} b_l e^{-j2\pi k \Delta f \tau^u_l} e^{j2\pi f^u_{D,l} b T_b} + \tilde{n}^{(1)}_{k,b}, \tag{16}$$

where $\kappa \triangleq \gamma \widetilde{\boldsymbol{w}}_c \boldsymbol{A}^{u,(1)}_R (\boldsymbol{A}^{u,(1)}_T)^H \widetilde{\boldsymbol{f}}_c$. According to (16), the estimation of distance and relative radial velocity can be transformed into a spectral estimation problem [4]. We apply two-dimensional FFT to $\boldsymbol{r}^{u,(1)}$ at step 2 by

$$(\boldsymbol{P}^{u,(1)})_{n,m} = \left| \sum_{k=1}^{K} \sum_{b=1}^{B} (\boldsymbol{r}^{u,(1)})_{k,b} e^{j2\pi \frac{nk}{K}} e^{-j2\pi \frac{mb}{B}} \right|^2. \tag{17}$$

We search for the maximum of $\boldsymbol{P}^{u,(1)}$ at step 3 and denote its index of row and column as Ω_d and Ω_v, respectively. Then the distance and relative radial velocity of the uth vehicle can be estimated at step 4 as

$$\hat{d}^u_{los} = \frac{\Omega_d}{K\Delta f}c, \quad \hat{v}^u_{los} = \frac{\Omega_v}{BT_b f_c}c. \tag{18}$$

Similarly, we can get $\boldsymbol{P}^{u,(2)}$ and $\boldsymbol{P}^{u,(3)}$ by applying two-dimensional FFT to $\boldsymbol{r}^{u,(2)}$ and $\boldsymbol{r}^{u,(3)}$, respectively at step 5. Next, we will estimate AoA and AoD of the LoS path using $(\boldsymbol{P}^{u,(1)})_{\Omega_d,\Omega_v}$, $(\boldsymbol{P}^{u,(2)})_{\Omega_d,\Omega_v}$ and $(\boldsymbol{P}^{u,(3)})_{\Omega_d,\Omega_v}$, which will be denoted as p_1, p_2 and p_3, respectively for simplicity of notation.

The relationship of $\boldsymbol{A}^{u,(1)}_R$ and $\boldsymbol{A}^{u,(2)}_R$ can be expressed as

$$\boldsymbol{A}^{u,(2)}_R = \boldsymbol{A}^{u,(1)}_R \Theta, \tag{19}$$

where $\Theta \triangleq \text{diag}\{[e^{j\pi\theta^{r,u}_1}, e^{j\pi\theta^{r,u}_2}, \cdots, e^{j\pi\theta^{r,u}_L}]\} \in \mathbb{C}^{L\times L}$.

It is shown in (19) that the rotation invariance property of the steering matrix, which is the basis of ESPRIT, so we can use p_1 and p_2 to estimate AoA of the LoS path. At step 6, by stacking p_1 and p_2 we get

$$\boldsymbol{P}^u \triangleq \begin{bmatrix} p_1 \\ p_2 \end{bmatrix} = \boldsymbol{R}\boldsymbol{T} + \widetilde{\boldsymbol{N}}, \tag{20}$$

where

$$\boldsymbol{R} \triangleq \begin{bmatrix} \gamma\widetilde{\boldsymbol{w}}_c \boldsymbol{A}^{u,(1)}_R \\ \gamma\widetilde{\boldsymbol{w}}_c \boldsymbol{A}^{u,(1)}_R \Theta \end{bmatrix} \in \mathbb{C}^{2\times L}, \boldsymbol{T} \triangleq \widetilde{\boldsymbol{\Delta}}(\boldsymbol{A}^{u,(1)}_T)^H \widetilde{\boldsymbol{f}}_c \in \mathbb{C}^{L\times 1}, \tag{21}$$

and $\widetilde{\boldsymbol{N}} \in \mathbb{C}^{2\times 1}$ is a noise vector by stacking the noise terms in p_1 and p_2. Let $\widetilde{\boldsymbol{\Delta}} \in \mathbb{C}^{L\times L}$ denotes a diagonal matrix with the two-dimensional FFT gain on the main diagnoal.

Since $\boldsymbol{R}\boldsymbol{T}$ is uncorrelated with $\widetilde{\boldsymbol{N}}$, we can obtain the autocorrelation of $\boldsymbol{P}^u$ at step 7 as

$$\boldsymbol{B}^u = \boldsymbol{P}^u (\boldsymbol{P}^u)^H \approx \boldsymbol{R}\left(\boldsymbol{T}\boldsymbol{T}^H\right)\boldsymbol{R}^H + \widetilde{\boldsymbol{N}}\widetilde{\boldsymbol{N}}^H. \tag{22}$$

The singular value decomposition of $\boldsymbol{B}^u$ at step 8 can be represented as

$$\boldsymbol{B}^u = \boldsymbol{U}\boldsymbol{\Sigma}\mathbf{U}^H, \tag{23}$$

where $\boldsymbol{U} \in \mathbb{C}^{2\times 2}$ denotes the unitary matrix and $\boldsymbol{\Sigma} \in \mathbb{C}^{2\times 2}$ denotes the real diagonal matrix with diagonal entries sorted in descending order. The first column of $\boldsymbol{U}$ corresponds to the largest diagonal entry of $\boldsymbol{\Sigma}$ and thus forms the LoS signal beamspace $\boldsymbol{U}_s$. Since $\boldsymbol{R}$ and $\boldsymbol{U}_s$ share the same basis, there exists a complex number T_R satisfying $\boldsymbol{U}_s = \boldsymbol{R}T_R$. We divide $\boldsymbol{U}_s$ into $U_{s,1}$ and $U_{s,2}$ at step 9 and have

$$\boldsymbol{U}_s = \begin{bmatrix} U_{s,1} \\ U_{s,2} \end{bmatrix} = \boldsymbol{R}T_R = \begin{bmatrix} \gamma\widetilde{\boldsymbol{w}}_c \boldsymbol{A}^{u,(1)}_R \\ \gamma\widetilde{\boldsymbol{w}}_c \boldsymbol{A}^{u,(1)}_R (\Theta)_{1,1} \end{bmatrix} T_R. \tag{24}$$

According to (24), we can get $U_{s,2} = U_{s,1}(\Theta)_{1,1}$. Then AoA of the LoS path can be estimated at step 10 as

$$\hat{\theta}^{r,u}_{los} = \arg(U_{s,2}/U_{s,1})/\pi. \tag{25}$$

As for the estimation of AoD of the LoS path, the relationship between $\boldsymbol{A}^{u,(1)}_T$ and $\boldsymbol{A}^{u,(3)}_T$ can be expressed as

$$\boldsymbol{A}^{u,(3)}_T = \boldsymbol{A}^{u,(1)}_T \Xi, \tag{26}$$

where $\Xi \triangleq \text{diag}\{[e^{j\pi\theta^{t,u}_1}, e^{j\pi\theta^{t,u}_2}, \cdots, e^{j\pi\theta^{t,u}_L}]\} \in \mathbb{C}^{L\times L}$. Since (26) and (19) have the same structure, AoD can be estimated in the same way as that of AoA by replacing

$$[p_1, p_2, \widetilde{\boldsymbol{w}}_c, \boldsymbol{A}^{u,(1)}_R, \Theta, \widetilde{\boldsymbol{\Delta}}, \left(\boldsymbol{A}^{u,(1)}_T\right)^H, \widetilde{\boldsymbol{f}}_c, \hat{\theta}^{r,u}_{los}] \tag{27}$$

with

$$\begin{aligned}&[(p_1)^H, (p_3)^H, (\widetilde{\boldsymbol{f}}_c)^H, \boldsymbol{A}^{u,(1)}_T, \\ &\quad \Xi, (\widetilde{\boldsymbol{\Delta}})^H, (\boldsymbol{A}^{u,(1)}_R)^H, (\widetilde{\boldsymbol{w}}_c)^H, \hat{\theta}^{t,u}_{los}].\end{aligned} \tag{28}$$

Then these estimated parameters, including $\hat{d}^u_{los}$, $\hat{v}^u_{los}$ and $\hat{\theta}^{r,u}_{los}$ can be exploited to get $\boldsymbol{Z}[t]$ in the RSU.

B. Beam Tracking

For the simplicity of analysis, we describe the EKF beam tracking model in Cartesian coordinate system. We define the state vector for the uth vehicle at the tth epoch in the RSU as

$$\boldsymbol{x}[t] \triangleq [x, y, v_x, v_y], \tag{29}$$

where x, y, v_x and v_y are denoted as the x-axis coordinate value, y-axis coordinate value, the velocity component in the x-axis direction and in the y-axis direction of the uth vehicle, respectively. Based on the geometric model shown in Fig. 1, the observation model can be derived as

$$\boldsymbol{Z}[t] = \begin{bmatrix} \sqrt{x^2+y^2} \\ \sin(\arctan(y/x)+\pi/2) \\ [y,x]\cdot([v_y,v_x])^T/\sqrt{x^2+y^2} \end{bmatrix} + \boldsymbol{z}_t, \tag{30}$$

where $\boldsymbol{z}_t$ is denoted as the observation noise satisfying Gaussian distribution with zero mean and variance matrix $\boldsymbol{Q}$. We denote the predicted state vector obtained at the $(t-1)$th epoch as $\overline{\boldsymbol{x}}[t]$. Then $\overline{\boldsymbol{x}}[t]$ and $\boldsymbol{Z}[t]$ are exploited by the EKF to obtain the filted state vector $\hat{\boldsymbol{x}}[t]$ at the tth epoch.

To adapt to the channel with high mobility and track the uth vehicel efficiently, at the $(t+1)$th epoch, the RSU should design the beamforming based on the predicted AoA. Based on the vehicle's kinematic equation, we can express the state revolution model as

$$\overline{\boldsymbol{x}}[t+1] = \begin{bmatrix} 1 & 0 & dt & 0 \\ 0 & 1 & 0 & dt \\ 0 & 0 & 1 & 0 \\ 0 & 0 & 0 & 1 \end{bmatrix} \hat{\boldsymbol{x}}[t], \tag{31}$$

where dt is the time interval of tracking and $\overline{\boldsymbol{x}}[t+1]$ is the predeicted state vector at the $(t+1)$th epoch. Then according to Fig. 1, the predicted AoA can be computed as

$$\overline{\theta}^{r,u}_{los} = \arctan((\overline{\boldsymbol{x}}[t+1])_2/(\overline{\boldsymbol{x}}[t+1])_1). \tag{32}$$

The obtained $\overline{\theta}^{r,u}_{los}$ can be exploited by the RSU to choose the beamforming codeword at the $(t+1)$th epoch. Similar procedure can be adopted by the vehicles to track the RSU by replacing AoA with AoD.

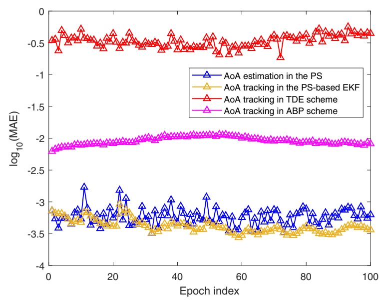

Fig. 2. Comparisons of MAE of AoA tracking for different schemes.

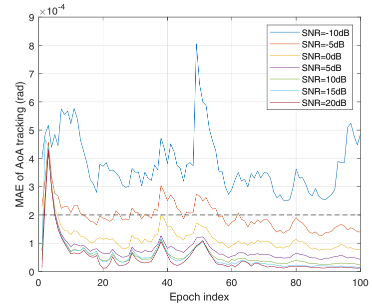

Fig. 3. Comparisons of MAE of AoA tracking for different SNR values.

IV. Simulation Results

Now we evaluate the performance of the proposed collaborative sensing and parameter estimation scheme in EKF beam tracking. Let us consider an mmWave MIMO ISAC system including a RSU and $U = 3$ vehicles where we set $N_r = 64$, $M_r = 4$, $N_t = 16$, $M_t = 2$ and $L = 3$. The mean power ratio between LoS path and non-LoS path is 10dB. We set $K = 316$, $\Delta f = 240$kHz, $T_o = 5.2$us and $f_c = 30$GHz in OFDM. During one epoch of tracking, each vehicle sends $B = 128$ OFDM blocks to the RSU and the time interval of tracking is set as $dt = 0.1$s.

We assume that one of the vehicles moves on the road at the instant velocity of $[20, 0]^T$m/s and its initial coordinate is set as $[-88, -100]^T$m. The coordinate of the RSU is set as $[0, 0]^T$m. All results are averaged from 2000 Mento Carlo simulations unless otherwise specified.

In Fig. 2, we compare the mean absolute error (MAE) of AoA tracking for the proposed scheme (PS), the two-dimensional ESPRIT (TDE) scheme in [8] and the auxiliary beam pair-based (ABP) beam tracking scheme in [9] at a signal-to-noise ratio (SNR) of -10dB. It is observed that the PS outperforms the existing schemes. Compared with the TDE scheme, On one hand, the PS takes advantage of the *a priori* information obtained from the last epoch of tracking and thus saves more estimation resourses. On the other hand, the power gain of the directional beams in the PS is higher than that of the omnidirectional beams in [8], leading to higher SNR gain and less estimation error. Furthermore, the performance of ABP scheme relies heavily on the beamwidth and when the angle varies rapidly, the SNR gain decreases, leading to worse tracking performance. The PS-based EKF tracking considers the distance and radial velocity and is less insensitive to the angle variation than the ABP scheme.

In Fig. 3, we compare the MAE of the PS for SNRs of -10, -5, 0, 5, 10, 15 and 20dB in terms of the epoch index. Obviously, higher SNR results in better tracking performance. Moreover, the PS-based EKF beam tracking can converge after about five epoches at high SNRs.

V. Conclusion

In this paper, we have proposed a collaborative sensing and parameter estimation scheme based on two-dimensional FFT and ESPRIT. Additionally, we have applied the PS in EKF to achieve beam tracking. Compared with [6], the PS-based tracking can distinguish different targets easily through pilot sequences. Compared with [8], the PS-based tracking can save much estimation resources at the guarantee of estimation accuracy. Compared with [9], the PS-based tracking can exploit the distance and radial velocity and become insensitive to the angle varition. Simulation results have verified the effectiveness of our scheme. Future work will focus on developing sensing algorithms that are computationally efficient.

Acknowledgment

This work is supported in part by National Natural Science Foundation of China (NSFC) under Grant 62071116, and by National Key Research and Development Program of China under Grant 2021YFB2900404.

References

[1] J. A. Zhang, F. Liu, C. Masouros, R. W. Heath, Z. Feng, L. Zheng, and A. Petropulu, "An overview of signal processing techniques for joint communication and radar sensing," *IEEE J. Sel. Topics Signal Process.*, vol. 15, no. 6, pp. 1295–1315, Nov. 2021.

[2] S. D. Liyanaarachchi, C. B. Barneto, T. Riihonen, and M. Valkama, "Joint OFDM waveform design for communications and sensing convergence," in *Proc. IEEE Int. Conf. on Commun. (ICC), Dublin, Ireland*, Jun. 2020, pp. 1–6.

[3] C. Qi, W. Ci, J. Zhang, and X. You, "Hybrid beamforming for millimeter wave MIMO integrated sensing and communications," *IEEE Commun. Lett.*, vol. 26, no. 5, pp. 1136–1140, Mar. 2022.

[4] J. A. Zhang, X. Huang, Y. J. Guo, J. Yuan, and R. W. Heath, "Multibeam for joint communication and radar sensing using steerable analog antenna arrays," *IEEE Trans. Veh. Technol.*, vol. 68, no. 1, pp. 671–685, Jan. 2019.

[5] F. Liu and C. Masouros, "A tutorial on joint radar and communication transmission for vehicular networks—part III: Predictive beamforming without state models," *IEEE Commun. Lett.*, vol. 25, no. 2, pp. 332–336, Sep. 2020.

[6] W. Yuan, F. Liu, C. Masouros, J. Yuan, D. W. K. Ng, and N. González-Prelcic, "Bayesian predictive beamforming for vehicular networks: A low-overhead joint radar-communication approach," *IEEE Trans. Wireless Commun.*, vol. 20, no. 3, pp. 1442–1456, Mar. 2021.

[7] C. Qi, P. Dong, W. Ma, H. Zhang, Z. Zhang, and G. Y. Li, "Acquisition of channel state information for mmWave massive MIMO: Traditional and machine learning-based approaches," *Sci. China Inf. Sci.*, vol. 64, no. 8, pp. 1–16, Aug. 2021.

[8] W. Ma, C. Qi, and G. Y. Li, "High-resolution channel estimation for frequency-selective mmWave massive MIMO systems," *IEEE Trans. Wireless Commun.*, vol. 19, no. 5, pp. 3517–3529, May 2020.

[9] D. Zhu, J. Choi, and R. W. Heath, "Auxiliary beam pair enabled AoD and AoA estimation in closed-loop large-scale millimeter-wave MIMO systems," *IEEE Trans. Wireless Commun.*, vol. 16, no. 7, pp. 4770–4785, May 2017.